Optics Communications 284 (2011) 4642–4645

Contents lists available at ScienceDirect

Optics Communications

journal homepage: www.elsevier.com/locate/optcom

Albedo and gain threshold of a diffusive Raman random laser ☆

A.C. Selden

20 Wessex Close, Faringdon, Oxfordshire, SN7 7YY, United Kingdom

ARTICLE INFO

Article history:
Received 14 January 2011
Received in revised form 24 May 2011
Accepted 13 June 2011
Available online 25 June 2011

Keywords:
Random laser
Raman scattering
Diffusion
Albedo

ABSTRACT

The diffuse reflectance (albedo) and transmittance of a Raman random gain medium are derived from a diffusion equation with power dependent gain. The results show good agreement with the experimental data for barium nitrate powder. Both the Raman albedo A_R and Raman transmittance T_R diverge at a critical gain γ_c, interpreted as the threshold for diffusive Raman laser generation. The parametric dependence of the albedo and threshold gain on the scattering characteristics of the random medium is analysed and the feedback effect of Fresnel reflection at the gain boundaries evaluated. The addition of external mirrors, particularly at the pumped surface, significantly reduces the generation threshold.

1. Introduction

A number of non-linear optical effects have been observed in random laser media via the enhanced interaction arising from multiple scattering and gain, namely second and higher harmonic generation [1–3], anti-Stokes random lasing [4], up-conversion lasing [5], stimulated Raman scattering [6] and surface plasmon enhanced Raman scattering [7] and random lasing [8]. Raman random lasing has been reported in SiC nanorods [9] and the Raman random laser threshold evaluated for a cloud of cold atoms [10], while the feasibility of Raman laser generation in powder media is supported by current developments in CW solid state Raman laser technology [11]. Raman gain has indeed been observed in optically pumped barium nitrate powder via the enhanced reflectance and transmission gain of a Raman probe beam [12]. Unlike conventional random lasers, which function by optical excitation via the absorption bands, Raman random laser media require no intrinsic absorption, but operate by non-linear conversion of the pump light. As such they are ideally lossless, any residual absorption arising from impurities and surface contamination, thereby enabling the pump flux to reach much greater depths than in optically pumped random lasers. Raman gain observed in mono-crystalline barium nitrate powder has been modelled as a radiative transfer process in a scattering medium with non-uniform gain using Monte Carlo methods, the gain profile being determined from the observed variation of pump intensity with optical depth [12]. The pump radiation penetrates to a depth ~2 mm, equivalent to ~20 scattering lengths in a layer of randomly packed cubic crystals ~0.2–0.3 mm in size. A linear analysis of the propagation of light in powdered laser media has previously been made using the Kubelka–Munk two-flux equations with constant coefficients [13] and the dynamics of dye and powder random lasers modelled using time-dependent diffusion equations [14,15]. Diffusion analysis has also been applied to model two-photon absorption in a random medium [16] and the distribution of second harmonic light in porous GaP [2]. Here we apply diffusion theory to analyse Raman gain in a random medium, finding quantitative agreement with the experimental data for the diffuse reflectance and transmittance gain of barium nitrate powder [12]. Having validated the diffusion analysis, we apply it to determine the parametric dependence of the Raman albedo and Raman random laser threshold on the scattering characteristics of a random gain medium, with feedback provided by Fresnel and specular reflection of diffuse light at the gain boundaries [17,18].

2. Diffusion theory

In the original experiment, a laser pump beam and a Raman shifted probe beam were coincident on a sample of mono-crystalline barium nitrate powder, the interaction of the strong pump radiation diffusing into the sample with the diffuse Raman probe radiation providing Raman gain via non-linear conversion of the pump radiation [12]. The process is modelled here via coupled diffusion equations in a 1D planar geometry, with the spatial distribution of the Raman gain determined by the diffuse pump flux distribution.

The diffusion equation for the scalar pump flux φ_p is

$$\partial^2\varphi_p + S_p(\tau) = \kappa^2\varphi_p \tag{1}$$

where $\partial^2\varphi_p = d^2\varphi_p/d\tau^2$, $d\tau = \kappa_e dz$, κ_e is the extinction coefficient, z is the spatial coordinate, $S_p(\tau)$ the source function (attenuated pump beam) and the diffuse attenuation parameter κ is defined by

☆ Research carried out while the author was a Visiting Professor in the Dept of Physics at the University of Zimbabwe, Mount Pleasant, MP 167, Harare, Zimbabwe.

E-mail address: adrian_selden@yahoo.com.

0030-4018/$ – see front matter © 2011 Elsevier B.V. All rights reserved.
doi:10.1016/j.optcom.2011.06.021

$\kappa^2 = 3(1-\varpi)(1-\varpi g)$, where $\varpi = \kappa_s/\kappa_e$ is the particle scattering albedo, κ_s is the scattering coefficient, the extinction coefficient $\kappa_e = \kappa_s + \kappa_a$, κ_a is the absorption coefficient and g the scattering asymmetry [19]. The equation for the diffuse Raman radiation flux φ_R in the Raman gain medium is

$$\partial^2\varphi_R + S_R(\tau) + B_R^2(\tau)\varphi_R = 0 \tag{2}$$

where $S_R(\tau)$ is the source function (attenuated Raman probe beam) and $B_R^2(\tau) \approx 3\gamma(\tau)(1-\varpi g)$ for $\varpi \approx 1$ [20]; $\gamma(\tau) = \gamma_R(\tau)\lambda_s$ is the dimensionless Raman gain parameter, $\gamma_R(\tau)$ is the spatially varying Raman gain coefficient, the scattering length $\lambda_s = 1/\kappa_s$ and $\gamma_R(\tau) = \Gamma_R\varphi_p(\tau)$, where Γ_R is the intensity dependent Raman gain [12] and $\varphi_p(\tau)$ the pump flux distribution. Eqs. (1) and(2) are coupled diffusion equations describing Raman diffusion in the random gain medium. Setting $S_R(\tau) = 0$ in Eq. (2) yields the diffusive Raman laser threshold equation [21]

$$\partial^2\varphi_R + B_R^2(\tau)\varphi_R = 0. \tag{3}$$

Eq. (1) can be solved analytically for a planar, normally incident pump beam, equivalent to an exponentially decaying source in the scattering medium [2], to yield the diffuse pump flux distribution

$$\varphi_p(\tau) = \varphi_0\left[e^{-\kappa\tau} - \alpha e^{-\kappa(2\Lambda-\tau)} - \beta e^{-\tau}\right] \tag{4}$$

from which the spatially varying Raman gain profile $\gamma_R(\tau)$ is derived. The second term in Eq. (4) accounts for reflection of the diffuse flux at the rear boundary, where $\Lambda = L/\lambda_s$, L is the physical thickness of the random medium, λ_s is the scattering length and the coefficients α and β are determined from the boundary conditions. When applied to diffusion in the powder layer, the fluxes φ_p and φ_R are extrapolated to zero a distance τ_e (extrapolation distance) beyond the boundary, determined by the refractive index n ($\tau_e = 2.42$ for $n = 1.5$ [16,22]). For anisotropic scattering, τ_e is expressed in terms of the transport length $\lambda_{tr} = \lambda_s/(1-\varpi g)$ [22]. For a perfectly reflecting boundary τ_e is infinite and the slope zero: $\partial\varphi|_{\tau=0} = 0$. A diffusing layer with one perfectly reflecting boundary is mathematically equivalent to a slab of twice the width, with identical boundaries and a scalar flux distribution $\varphi(\tau)$ symmetric about the mid-plane.

Eq. (2) is used to determine the diffuse Raman reflectance (Raman albedo) A_R and Raman transmittance T_R of the powder layer from the diffuse emission (radiance) at the boundaries: $J_R(0,\Lambda) = -D\partial\varphi_R|_{\tau=0,\Lambda}$ (D is the diffusion coefficient), which can be expressed in terms of the scalar fluxes $\varphi_R(0,\Lambda)$ via the boundary conditions [23]

$$\tau_e\partial\varphi_R|_{\tau=0,\Lambda} = \pm\varphi_R(0,\Lambda) \tag{5}$$

The observed gains in Raman albedo and diffuse Raman transmittance [12] are found from the ratios of the boundary fluxes evaluated with and without the pump source i.e. with and without Raman gain, for a fixed Raman probe intensity, on applying Eq. (5)

$$G(A_R) = J_R(0,\gamma_R)/J_R(0,0) = \varphi_R(0,\gamma_R)/\varphi_R(0,0) \tag{6a}$$

and

$$G(T_R) = J_R(\Lambda,\gamma_R)/J_R(\Lambda,0) = \varphi_R(\Lambda,\gamma_R)/\varphi_R(\Lambda,0) \tag{6b}$$

3. Results

3.1. Raman albedo

Calculations were made for planar pump and Raman probe beams incident on barium nitrate powder sandwiched between glass plates, for sample thicknesses in the range $L = 10$–$100\ \lambda_s$, as described in [12]. Raman gains were obtained from the ratios of transmitted and reflected Raman fluxes with and without Raman gain (Eqs. (6a, 6b)). The contribution of the diffuse pump flux reflected at the rear boundary was included in the gain profile (Eq. (4)). For the barium nitrate powder samples used in the experiment, the inferred scattering parameters were $\lambda_s \approx 110\ \mu m$ and $g \approx 0.7$; the Raman gain coefficient ranged from $\gamma_R = 0.5\ cm^{-1}$ to $2.2\ cm^{-1}$[12]. A small but positive enhancement of the Raman albedo of the powder at the lowest Raman gain sets a lower limit on the particle scattering albedo viz. $\varpi \geq 1-\gamma_R\lambda_s \geq 0.995$. For high particle scattering albedoes, both pump and probe beams penetrate further into the diffusive medium, sampling relatively large gain volumes, the diffuse Raman radiation flux reaching its maximum value ~10–20 scattering lengths from the pumped surface. Thus quite modest Raman gain can result in significant amplification of the multiply scattered Raman radiation, as shown by the enhanced diffuse reflectance and transmittance observed for barium nitrate powder [12]. Calculations of the Raman albedo gain $G(A_R)$ and diffuse Raman transmission gain $G(T_R)$ vs. L generate profiles with closely similar characteristics to those observed (Fig. 1), except for the quasi-exponential rise observed for thin powder layers ($L \leq 2$ mm). However, the value of the gain parameter γ_0 required to fit the data points is lower than the experimental value as a result of the one-dimensional nature of the analysis, which neglects lateral diffusion of scattered light within the finite gain volume [12].

Increasing the Raman gain by further increasing the incident pump intensity causes the diffusely reflected and transmitted fluxes to rise rapidly, the albedo gain $G(A_R)$ and transmittance gain $G(T_R)$ diverging as the Raman gain parameter γ approaches a critical value γ_c, interpreted as the threshold gain parameter γ_{th} for diffusive Raman laser generation. Fig. 2 shows plots of the albedo gain GA_R vs. gain parameter γ_0 for several values of scattering asymmetry g. However, the gain ratio $G(T_R)/G(A_R)$ remains finite, reaching a limiting value when $\gamma = \gamma_{th}$.

3.2. Raman laser threshold

The Raman laser threshold condition (Eq. (3)) is satisfied for a specific value of the Raman gain parameter $\gamma_0 = \gamma_{th}$ given by the eigenvalue $B_0^2 \approx 3\gamma_0(1-\varpi g)$ [21]. The dependence of γ_{th} on the depth of the powder layer and the boundary conditions e.g. reflecting boundaries, is found by numerical solution of Eq. (3), with the gain profile $\gamma(\tau)$ determined by the diffuse pump flux distribution $\varphi_p(\tau)$. For uniform gain $B_R^2 = B_0^2$ constant, $B_0 = \pi/(\Lambda + 2\tau_e)$ and $\gamma_0 \approx \pi^2/3(1-\varpi g)(\Lambda + 2\tau_e)^2$[21], where we have included the extrapolation distance τ_e at the boundaries [17,22,23].

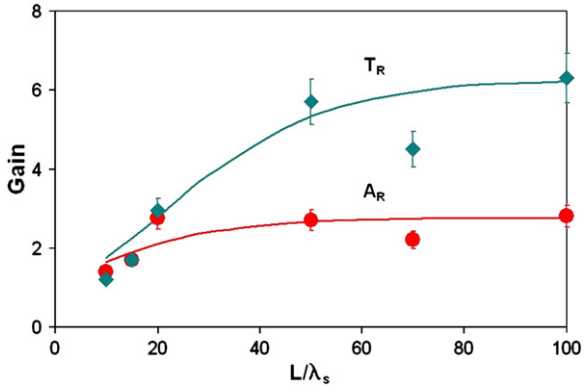

Fig. 1. Raman albedo A_R and Raman transmission gain T_R of barium nitrate powder vs. thickness L of the powder layer for $\varpi = 0.995$, $g = 0.7$. The theoretical curves are matched to the experimental data points ●, ♦ by adjusting the gain parameter γ_0. The albedo saturates at smaller depths than the transmission gain, as observed.

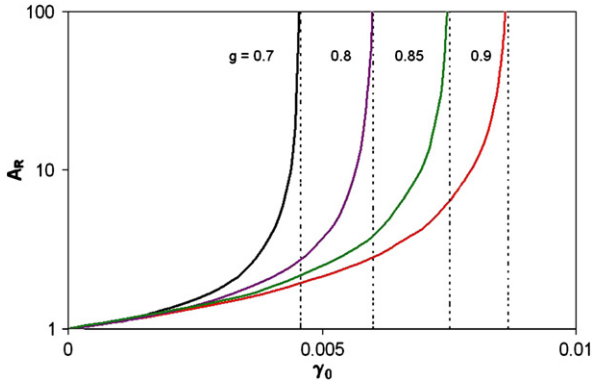

Fig. 2. Raman albedo A_R vs. Raman gain parameter γ_0 for selected values of the scattering asymmetry g, the albedo increasing without limit as γ_0 approaches the threshold gain γ_{th} (indicated by vertical dotted lines). Plane layer ($L=20\lambda_s$, $\varpi=1$) with 100% reflector at rear boundary.

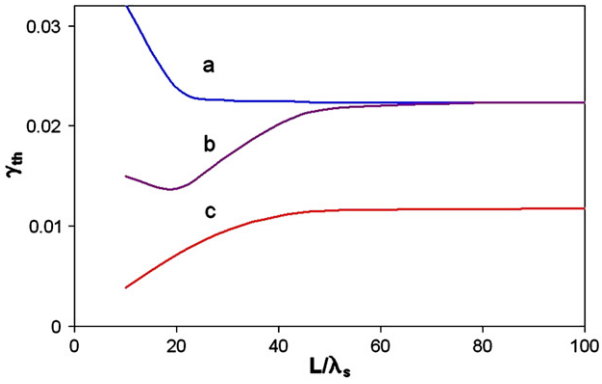

Fig. 4. Threshold gain parameter $\gamma_{th}=\gamma_R\lambda_s$ vs. powder layer thickness L/λ_s expressed in units of scattering length λ_s ($\varpi=0.995$, $g=0.7$). The curves compare the influence of boundary reflectance on threshold gain: (a) powder layer between glass slides, (b) 100% reflector at rear boundary, and (c) 100% reflectors at both boundaries.

For random gain media with high particle scattering albedo (low absorption loss), the diffuse pump flux φ_p extends further into the gain medium. This is illustrated in Fig. 3, which shows the pump flux profiles for a powder layer with total reflection at one boundary, the profile becoming flat i.e. uniform gain, when $\varpi=1$ (zero absorption). However, the threshold Raman flux profiles span a rather narrow range, approximating the ideal constant gain case, although the threshold gain varies by a factor ≈ 3 (Fig. 3 inset).

The Raman laser threshold is significantly reduced with feedback provided by external mirrors, as observed for optically pumped random lasers [18,24]. A 100% reflector at the rear boundary reduces the threshold for the thinner layers, the lowest threshold (~50% reduction) being reached when $L/\lambda_s=20$, but its effect disappears when $L/\lambda_s>50$ (Fig. 4). A 100% reflector situated at the pumped surface has the maximum effect [25], halving the threshold for the thick powder layers ($L/\lambda_s>50$). The lowest threshold occurs for the thinner layers with 100% reflectors at both boundaries, where both contribute to the feedback.

The dependence of the threshold gain parameter $\gamma_{th}=\gamma_R\lambda_s$ on particle scattering albedo ϖ and scattering asymmetry g is shown in Fig. 5, γ_{th} decreasing rapidly as ϖ increases i.e. as the loss per scattering diminishes; it shows a weaker dependence on scattering asymmetry g, slowly decreasing as g increases, except for $\varpi=1$ (perfect scattering), when the boundary reflectance is dominant. The threshold gain parameter $\gamma_{th}=\gamma_R\lambda_s$ is plotted against the diffuse attenuation parameter $\kappa=\kappa_d\lambda_s$ for the pump flux in Fig. 6, showing the monotonic increase in threshold gain with increased attenuation of the diffuse pump radiation. The dashed curves are power law fits to the data points of the form $y=a+bx^n$, where a, b, n are constants and $x=\kappa_d\lambda_s$. The exponent n lies in the range $1.76\le n\le 1.96$, consistent with diffusion theory ($n=2$), for which the threshold gain parameter scales as $\gamma_{th}\propto(\lambda_s/\lambda_d)^2$, where $\lambda_d=1/\kappa_d$ is the diffusion length.

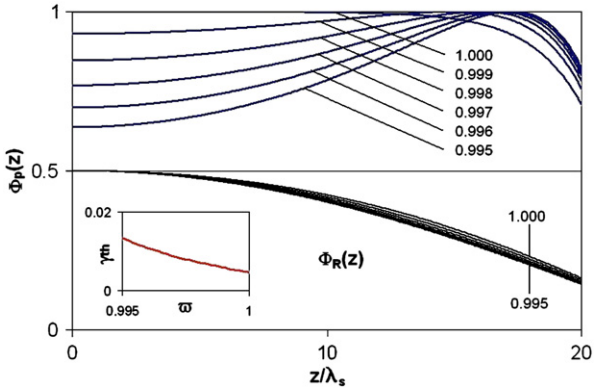

Fig. 3. Pump flux profiles $\varphi_p(z)$ for a layer with perfectly reflecting boundary, showing the convergence to a flat profile (uniform gain) for $\varpi=1$. Curves labelled with values of $\varpi=0.995$–1.000. Lower curves: Raman threshold flux profiles $\varphi_R(z)$ ($L/\lambda_s=20$, $g=0.7$). Inset: threshold gain parameter γ_{th} vs. scattering albedo ϖ.

4. Discussion

Given the simplicity of the diffusion analysis, it is satisfying that good qualitative agreement is found between the experimental and theoretical characteristics of the Raman albedo and transmission gain of barium nitrate powder. By adjusting the value of the single particle scattering albedo ϖ, the z-dependence of the pump flux profile is reproduced [12]; this value of ϖ is then used to calculate the Raman gain profiles, with appropriate re-scaling to account for the narrow forward diffraction lobe of the particle scattering pattern (phase function). As a result of the high scattering albedo ($\varpi\ge 0.995$), both pump and probe light diffuse into the depths of the powder layer, such that for the thinner layers Fresnel reflection of the diffuse flux at both boundaries has to be taken into account. An obvious refinement of the analysis would be to include the effect of the radial gain profile corresponding to the Gaussian profile of the incident pump beam, which diffuses laterally with increasing depth [12], and radial diffusion of the Raman radiation in the 'tear-drop' gain volume, as in a recent diffusion model of a dye random laser [26]. In addition, we note that a gain threshold for diffusive Raman laser action in barium nitrate powder is predicted by the analysis, analogous with laser generation via feedback scattering in random media [14,21].

The Raman laser threshold equation (Eq. (3)) is equivalent to Letokhov's threshold equation for random lasing, which derives from

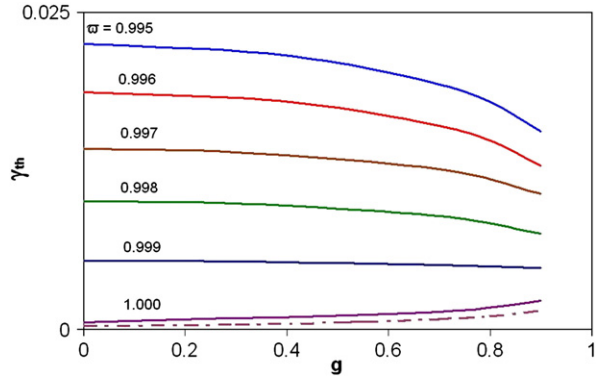

Fig. 5. Dependence of the threshold gain parameter γ_{th} on particle scattering albedo ϖ and scattering asymmetry g, showing the threshold reduction as $\varpi\Rightarrow 1$. The constant gain case is indicated by the lowest (dashed) curve [21].

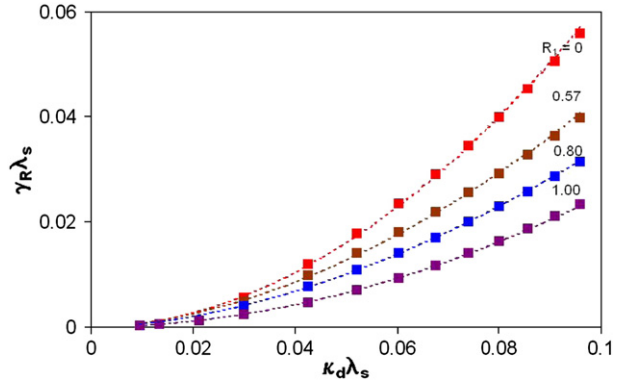

Fig. 6. Threshold gain parameter $\gamma_{th} = \gamma_R\lambda_s$ vs. diffuse attenuation parameter $\kappa_d\lambda_s$ for a range of boundary reflectance: $R_b = 0, 0.57, 0.80, 1.00$, showing the monotonic increase in threshold with increasing attenuation. Power law curves with exponents n in the range $1.8 \leq n \leq 2$ (consistent with diffusion theory) provide good fits to the calculated data points.

the criticality condition for diffusive neutron transport [21]; it is applied here for non-uniform gain (corresponding to the non-uniform pump flux profile). Noginov et al. analyse exponentially decreasing gain, but rely on numerical solution of the laser equation [14]. The source-free solution applies to the diffusive Raman laser threshold; for the albedo analysis the Raman probe beam is represented by including a source term in the non-linear Raman diffusion equation (Eq. (2)), the solution of which diverges (becomes infinite) as the gain approaches a critical gain γ_c, equal to the threshold gain γ_{th} found from Eq. (3).

The nature of laser generation in random media and its correct theoretical description is a topic of ongoing research [14,27], such that a Raman random laser could best be demonstrated by experiment [9,10]. However, the success of the diffusion model in analysing the Raman gain probe data for barium nitrate powder is encouraging and suggests it should be further tested against the experimental data for other non-linear media. The parametric dependence of the Raman random laser threshold is of particular interest, as this tends to be model-dependent. The reduction in gain threshold predicted for powders with near-perfect scattering ($\varpi \approx 1$), and a significant reduction with reflecting boundaries, particularly at the pumped surface, augur well for low threshold Raman powder lasers. The gain threshold also decreases for particles with higher scattering asymmetry i.e. larger particles, which could be tested by experiment [28]. The quasi-exponential increase in Raman albedo with depth observed for the thinner powder layers ($L \leq 2$ mm) is not explained by the diffusion analysis (nor by the Monte Carlo simulation) of stimulated Raman emission, suggesting that an alternative interpretation may be required in this regime, perhaps optical coupling via internal resonances in individual crystallites [29,30].

5. Conclusion

Diffusion analysis of the diffuse reflectance (Raman albedo) and transmittance of a Raman random gain medium gives good agreement with the experimental data for laser pumped barium nitrate powder [12]. A gain threshold for diffusive Raman laser generation in a random medium is predicted on the basis of the analysis, which could be tested by experiment. The parametric dependence of the Raman laser threshold on particle scattering albedo ϖ, scattering asymmetry g and diffuse attenuation parameter $\kappa = \kappa_d\lambda_s$ has been determined and the reduction in gain threshold achieved by the addition of external reflectors evaluated. The low intrinsic absorption loss associated with Raman random gain media allows order of magnitude increased penetration depths and interaction lengths compared with conventional optically pumped random lasers. As such, they enable stimulated Raman studies to be extended to mesoscopic random media, as is the case for second and higher harmonic generation [2,3].

References

[1] M.A. Noginov, S.U. Egarievwe, N. Noginova, J.C. Wang, H.J. Caulfield, J. Opt. Soc. Am. B 15 (1998) 2854.
[2] S. Faez, P.M. Johnson, D.A. Mazurenko, Ad Lagendijk, J. Opt. Soc. Am. B 26 (2009) 235.
[3] S.O. Konorov, D.A. Sidorov-Biryukov, I. Bugar, J. Kova, L. Fornarini, M. Carpanese, M. Avella, M.E. Errico, D. Chorvat Jr., J. Kova Jr., R. Fantoni, D. Chorvat, A.M. Zheltikov, Appl. Phys. B 78 (2004) 73.
[4] G. Zhu, C.E. Small, M.A. Noginov, Opt. Lett. 33 (2008) 920.
[5] H. Fujiwara, K. Sasaki, J. Jap. Appl. Phys. 43 (2004) L1337.
[6] V.P. Yashchuk, E.A. Tikhonov, O.A. Prigodiuk, JETP Lett. 91 (2010) 174.
[7] N.M. Lawandy, Appl. Phys. Lett. 85 (2004) 5040.
[8] G.D. Dice, S. Mujumdar, A.Y. Elezzabi, Appl. Phys. Lett. 86 (2005) 131105.
[9] H. Zhang, Z. Xu, H. Xu, C. Zhu, Chin. J. Lumin. 22 (2001) 66.
[10] W. Guerin, N. Mercadier, D. Brivio, R. Kaiser, Opt. Express 17 (2009) 11326.
[11] L. Fan, Y.X. Fan, H.T. Wang, Appl. Phys. B 101 (2010) 493.
[12] A.E. Perkins, N.M. Lawandy, Opt. Commun. 162 (1999) 191.
[13] M.A. Noginov, N. Noginova, S. Egarievwe, J.C. Wang, M.R. Kokta, J. Paitz, Opt. Mater. 11 (1998) 1.
[14] M.A. Noginov, J. Novak, D. Grigsby, L. Deych, J. Opt. A Pure Appl. 8 (2006) S285.
[15] D.S. Wiersma, Ad Lagendijk, Phys. Rev. E 54 (1996) 4256.
[16] A.L. Burin, H. Cao, M.A. Ratner, IEEE J. Sel. Top. Quantum Electron. 9 (2003) 124.
[17] J.X. Zhu, D.J. Pine, D.A. Weitz, Phys. Rev. A 44 (1991) 3948.
[18] M.A. Noginov, G. Zhu, C. Small, J. Novak, Appl. Phys. B 84 (2006) 269.
[19] R.M. Goody, Y.L. Yung, Atmospheric Radiation Pt. I, 2nd edn. O.U.P., 1989.
[20] A.C. Selden, J. Opt. A Pure. Appl. Opt. 2 (2000) 510.
[21] V.S. Letokhov, J. Exp. Theor. Phys. 26 (1968) 835.
[22] R. Aronson, J. Opt. Soc. Am. A 12 (1995) 2532.
[23] D.J. Durian, J. Rudnick, J. Opt. Soc. Am. A 16 (1999) 837.
[24] P.C. de Oliveira, J.A. McGreevy, N.M. Lawandy, Opt. Lett. 22 (1997) 700.
[25] Y. Feng, K. Ueda, Phys. Rev. A 68 (2003) 025803.
[26] R.G.S. El-Dardiry, A.P. Mosk, A. Lagendijk, Opt. Lett. 35 (2010) 3063.
[27] H.E. Türeci, Ge Li, S. Rotter, A.D. Stone, Science 320 (2008) 643.
[28] M.A. Noginov, G. Zhu, A.A. Frantz, J. Novak, S.N. Williams, I. Fowlkes, J. Opt. Soc. Am. B 21 (2004) 191.
[29] N.É. Ter-Gabriélyan, V.M. Markushev, V.R. Belan, C.M. Briskina, O.V. Dimitrova, V.F. Zolin, A.V. Lavrov, Sov. J. Quantum Electron. 21 (1991) 840.
[30] V.N. Astratov, S.P. Ashili, Opt. Express 15 (2007) 17351.